b) Diatomic gas $k=7/5$

Critical: $0 \le \frac{P_2}{P} \le \left(\frac{5}{6}\right)^{7/2}$

$$\tau = 7\left(\frac{P_2}{P}\right)^{1/7} \tag{14}$$

Subcritical: $\left(\frac{5}{6}\right)^{7/2} \le \frac{P_2}{P} \le 1$

$$\tau = \frac{7}{6}\sqrt{30} + \frac{175\sqrt{5}}{864}\left\{\frac{27\sqrt{6}}{50} - \left[\left(\frac{P_2}{P}\right)^{-2/7} + \frac{3}{2}\right]\right.$$
$$\times \left(\frac{P_2}{P}\right)^{-1/7}\left[\left(\frac{P_2}{P}\right)^{-2/7} - 1\right]^{1/2}$$
$$\left. + \frac{3}{4}\ell n \frac{(7/10)+\sqrt{6}/5}{(P_2/P)^{-2/7} - 1/2 + (P_2/P)^{-1/7}[(P_2/P)^{-2/7}-1]^{1/2}}\right\} \tag{15}$$

3) Isothermal venting

a) Monatomic gas, $k=5/3$

Critical: $0 \le \frac{P_2}{P} \le \left(\frac{3}{4}\right)^{5/2}$

$$\tau = \ell n \frac{P_2}{P} \tag{16}$$

Subcritical: $\left(\frac{3}{4}\right)^{5/2} \le \frac{P_2}{P} \le 1$

$$\tau = \frac{5}{2}\ell n \frac{3}{4} + \frac{5\sqrt{3}}{16}\left\{\frac{10\sqrt{3}}{9} - \left[\left(\frac{P_2}{P}\right)^{-2/5} + 2\right]\right.$$
$$\left. \times \left[\left(\frac{P_2}{P}\right)^{-2/5} - 1\right]^{1/2}\right\} \tag{17}$$

b) Diatomic gas, $k=7/5$

Critical: $0 \le \frac{P_2}{P} \le \left(\frac{5}{6}\right)^{7/2}$

$$\tau = \ell n \frac{P_2}{P} \tag{18}$$

Subcritical: $\left(\frac{5}{6}\right)^{7/2} \le \frac{P_2}{P} \le 1$

$$\tau = \frac{7}{2}\ell n \frac{5}{6} + \frac{175\sqrt{5}}{648}\left\{\frac{88\sqrt{5}}{125} - \left[3\left(\frac{P_2}{P}\right)^{-4/7}\right.\right.$$
$$\left.\left. -4\left(\frac{P_2}{P}\right)^{-2/7} + 4\right]\left[\left(\frac{P_2}{P}\right)^{-2/7} - 1\right]^{1/2}\right\} \tag{19}$$

Discussion

Equations (10) and (11) calculated for $k=5/3$ and 7/5 agree with Fig. 3.10.5a of Ref. 2. So do Eqs. (7–10) with Fig. 3.10.5b. However, Eqs. (16–19) do not agree exactly with Fig. 3.10.5c of Ref. 2. Mainly, there should be only one single curve for the critical flow. Consider example 3 on p. 17 of Ref. 3, which involves both critical and subcritical flow. Find the time t required to charge isothermally a $V=10$ ft^3 ullage at $P_i=14.7$–$P_f=40$ psia, using nitrogen $k=7/5$, $R=662$ in.-lb/lb·°R with an upstream pressure of $P_1=45$ psia and a temperature of $T_1=70°F=530°R=T_i$, given an effective flow area $C_DA_T=5.94$ in.^{2} From Eq. (9a), $C=0.365$ s; from Eq. (10), $\tau_i=0.327$; from Eq. (11), $\tau_f=0.938$; and from Eq. (8), $t=0.223$ s. Note that the values from Fig. 3 of Ref. 3 are given as $\tau_i=0.321$ and 0.923, respectively. As a result, $t=0.222$ s, which constitutes very close agreement.

Acknowledgment

The author wishes to thank Mr. Chor K. Tan for bringing Refs. 2 and 3 to his attention.

References

[1] Shapiro, A. H., *The Dynamics and Thermodynamics of Compressible Flow*, Vol. 1, Ronald Press Co., New York, 1953, p. 110.

[2] Howell, G. W. and Weathers, T. M., "Aerospace Fluid Component Designers' Handbook," U.S. Air Force Rocket Propulsion Laboratory, Edwards, CA, PRL-TDR-64-25, May 1964, Feb. 1970.

[3] Thompson, W. and Nepo, F. (R.E.), "Analysis, Design and Development of High-Flow Helium Pressure Regulator," Vol. 2, Robertshaw Controls Co., Anaheim, CA, Rept. AFBMD-TR-60-72 (II), June 1960.

Separated Flow Treatment with a New Turbulence Model

Uriel C. Goldberg*
Rockwell International Science Center
Thousand Oaks, California

Nomenclature

k = kinetic energy of turbulence
n,s = coordinates locally normal and parallel to the wall, respectively
u_s = velocity scale for separated flows
u_t = locally tangential mean velocity component
u_τ = wall friction velocity scale
ϵ = isotropic part of turbulence energy dissipation
κ = von Kármán constant, = 0.4
ν = kinematic molecular viscosity
ν_t = kinematic eddy viscosity

Subscripts

b = backflow edge
v = viscous sublayer edge
w = wall

Introduction

MANY flowfields of practical importance involve regions where the flow detaches from a solid surface and reattaches further downstream, thereby forming a separation bubble. Most existing turbulence models either do not treat such bubbles or do so in an ad hoc fashion, which is frequently inadequate. The present work attempts to address this problem in a more rigorous manner, to enable improved turbulence modeling for separated regions.

From experimental investigations by Simpson et al.[1-3] of two-dimensional separated flows, the following features emerge: a) the backflow is governed by large-scale outer-region eddies, whose influence increases as the backflow develops downstream of detachment; b) the separating shear layer behaves progressively more like a free shear mixing

Received Nov. 19, 1985; revision received Jan. 8, 1986.

*Member of Technical Staff. Member AIAA.

layer in the streamwise direction, as it grows at a rate proportional to δ^2; c) the part of the backflow adjacent to the wall has little Reynolds stress effects; d) the Reynolds stresses within the backflow region are a product of the turbulence structure, not of the local mean velocity gradients; e) initial conditions, such as the upstream boundary layer, have little influence on the flow structure within the separated region; and f) the local maximum Reynolds shearing stress, occurring in the middle of a detached shear layer, is the proper stress scale for separated flows.

These phenomena were also observed by Délery[4] in his experiments on shock-induced separation in transonic flow.

The following k-ϵ model for wall-bounded separated flows is based on these observations. It also assumes that the viscous sublayer, which is adjacent to the wall upstream of separation and downstream of reattachment, is pushed away from the wall and fed by the backflow, while the turbulence behavior across it remains qualitatively unchanged from that upstream of separation. This limits the intended scope of the model to bubbles not large enough to significantly alter the inviscid far field.

Figure 1 shows a schematic view of a separation bubble, indicating the various locations and lines of significance to the model.

Model Formulation

k and ϵ are prescribed analytically between the wall and the backflow edge so that continuity in magnitude (for both) and slope (for k) is preserved as the formulation switches from the backflow region to the viscous sublayer (Fig. 1). This continuity requirement results from observation d above, suggesting that the backflow edge ($u_t = 0$ line), $n_b(s)$, bears no significance for k and ϵ.

k distribution in the backflow region is assumed to be Gaussian, similar to its behavior in a free shear mixing layer:

$$k/k_b = [e^{\phi}/(e^{\phi}-1)]\,[1-e^{-\phi(n/n_b)^2}] \equiv \mathcal{G}(s,n), \quad 0 \leq n \leq n_b \tag{1}$$

$\mathcal{G}$ must impose on k the same type of curvature within the backflow region as that within the viscous sublayer located outside of it, limiting ϕ to the range $0 < \phi \leq 0.50$. It is assumed that ϕ is not a function of s, so that a one-time parametric study will suffice to fix ϕ, making it an invariant of the model. The last assumption draws on observation e, which suggests that turbulence scales may be self-similar within the backflow, at least for bubble sizes considered herein.

In view of observation a, it is assumed that the length scale of turbulence in the backflow is proportional to n_b, namely, $L = \sigma(s) n_b(s)$, where $\sigma(s)$ is to be determined. This together with Eq. (1) establishes ϵ:

$$\epsilon = k^{3/2}/L = (\sigma n_b)^{-1}\,[k_b \mathcal{G}(s,n)]^{3/2}, \quad 0 \leq n \leq n_b \tag{2}$$

As shown in Ref. 5, $\epsilon = 2\nu_w k_v / n_v^2 = \text{const}$ across an attached viscous sublayer. As the sublayer becomes detached, ν_w may no longer influence ϵ, whose constant value across the sublayer now becomes $k_v^{3/2}/n_v$.

To enforce continuity of ϵ across $n_b(s)$, i.e., $\epsilon_{b^-} = \epsilon_{b^+}$, one must therefore impose $k_b^{3/2}/\sigma n_b = k_v^{3/2}/n_v$. Thus,

$$k_b = (\sigma n_b / n_v)^{2/3} k_v \tag{3}$$

For streamwise continuity of the formulation, n_v must include both attached and detached portions of the viscous sublayer:

$$n_v^* = 20 C_\mu^{1/4} + n_b^*, \quad n^* \equiv n u_s/\nu_w, \quad C_\mu = 0.09 \tag{4}$$

where $u_s = (\overline{-u'v'})_{\max}^{1/2} = [\nu_{t,m}(\partial u_t/\partial n)_{\max}]^{1/2}$. Here $(-u'v')_{\max}$ is the maximum Reynolds stress assumed to correspond to the maximum normal-to-wall mean velocity gradient. Some justification for this is found in Refs. 1 and 4. $\nu_{t,m}$ is the value of eddy viscosity where the aforementioned maximum gradient occurs (see Fig. 1). Since $\nu_{t,m}$ is not known initially, an iterative procedure may be necessary in which $\nu_{t,m}$ is updated from the solution of the k-ϵ equations. Equation (4) assumes that the formulation for the attached viscous sublayer thickness[5] is unchanged as the sublayer becomes detached.

Combining Eqs. (2) and (3) yields $\epsilon = [k_v \mathcal{G}(s,n)]^{3/2}/n_v$, $0 \leq n \leq n_b$. The boundary conditions for the high turbulence Reynolds number k-ϵ equations, set at the viscous sublayer edge are assumed to retain their attached-flow formulation,[5]

$$k_v = u_s^2/\sqrt{C_\mu^*}, \quad \epsilon_v = u_s^3/(\kappa n_v), \quad C_\mu^* = 0.7 \tag{5}$$

however, u_s replaces u_τ, which is inappropriate for separated flow regions and C_μ^* replaces C_μ.

The parabolic distribution of k across the viscous sublayer[5] is now given by

$$k = k_v - (k_v - k_b)(n_v^2 - n^2)/(n_v^2 - n_b^2), \quad n_b \leq n \leq n_v \tag{6}$$

which reduces to $k = k_v (n/n_v)^2$ (see Ref. 5) in the nonseparated sections of the flow, where both n_b and k_b vanish.

Imposing slope continuity on k across the $n_b(s)$ line, using Eqs. (1), (3), and (6), establishes σ as $\sigma(s) = (n_v/n_b)/\beta^{3/2}$, whence

$$L = n_v/\beta^{3/2} \tag{7a}$$

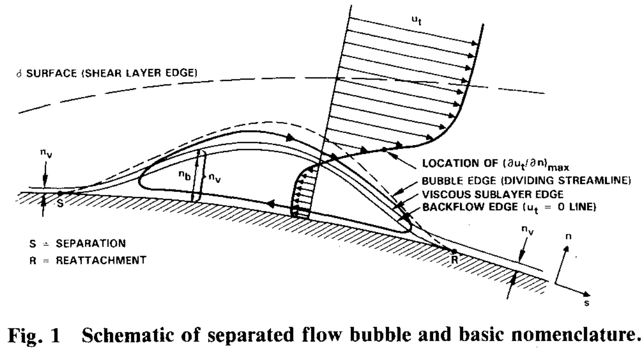

Fig. 1 Schematic of separated flow bubble and basic nomenclature.

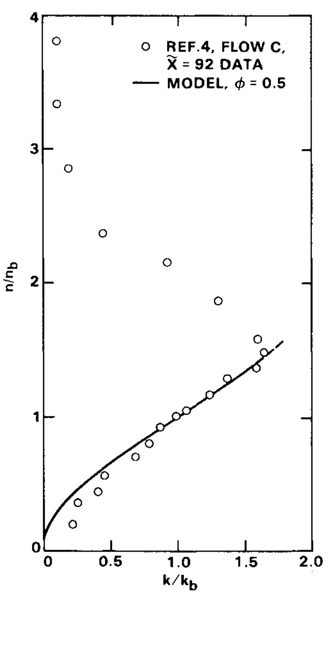

Fig. 2 Comparison between prediction and data of Ref. 4 for kinetic energy.

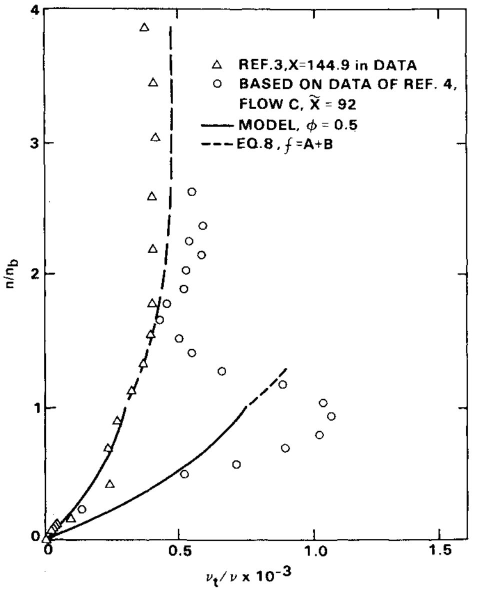

Fig. 3 Comparison between prediction and data of Refs. 4 and 3 for eddy viscosity.

where

$$\beta \equiv k_v/k_b = 1 + [(n_v/n_b)^2 - 1]\phi/(e^\phi - 1) \quad (7b)$$

Thus L is proportional to n_v, increasing as the backflow develops and decreasing toward reattachment, in agreement with observations a and b.

An eddy viscosity formula is now obtained from the following argument. As pointed out in Ref. 5, the basic relation $\nu_t = C_\mu k^2/\epsilon$ must be modified within the viscous sublayer to preserve the correct behavior $\nu_t \sim n^3$ at the wall, giving rise to the formula $\nu_t = C(n)k^2/(\epsilon n^+)$. In a similar manner, eddy viscosity within the backflow is assumed to be of the form $\nu_t = f(n)k^2/\epsilon$. Using Eqs. (1-5), and (7) yields

$$\nu_t/\nu_w = [f(n/n_b)/(2\sqrt{2}\beta^2)]\, n_v^* \mathcal{G}^{1/2}(s,n), \quad 0 \leq n \leq n_b \quad (8)$$

where

$$f(n/n_b) = A(n/n_b) + B,\ A = -(C_\mu^*/2)^{9/5},\ B = (C_\mu^*/2)^{3/5} - A$$

This form of f seems to best correlate with the data.[3,4]

The corresponding formula within the viscous sublayer is of the form $(\nu_t/\nu_w)_{sub} = C(n)[k^2/\nu\epsilon]_{sub}$, where k is given by Eq. (6) and $\epsilon = k_v^{3/2}/n_v$. Here, $C(n_b) = C_\mu^{*1/4}(A+B)/2\sqrt{2}$, A and B being given previously.

This concludes the formulation of the model, which ignores the viscous region adjacent to the wall within the separation bubble. This is justifiable in view of observation c.

Testing of Model

In order to test the model, arbitrary streamwise locations were selected from Ref. 4, flow C, $\tilde{x} = 92$, and from Ref. 3, $x = 144.9$ in. The two sets of data pertain to different geometries, initial conditions, and means by which flow separation was imposed. A large separation bubble existed in the flow of Ref. 4, and the chosen location is approximately in the middle of it. Figure 2 compares k from Eqs. (1) and (6), with the data. The agreement supports the Gaussian concept. Furthermore, calculated values of k_b at this and other locations were found to be within only 2% of those obtained from the measurements. Based on the measured velocity profile and shear stress distribution at the selected station, eddy-viscosity data were compared with Eq.(8), as shown in Fig. 3. Since the velocity profile had to be numerically treated to derive $\partial u/\partial y$, some error was introduced into the data points; nevertheless, the agreement is reasonable. In the case of Ref. 3, eddy viscosity was already given in data form. Figure 3 also shows comparison of ν_t prediction with these data at the selected location. Agreement is very good, even well beyond the backflow. In addition, predicted ν_t levels dropped about 45% when going from well upstream of separation into the bubble along a constant n, as experimentally observed.[3] This leads credibility to the length scale L. These tests serve as a preliminary validation of the model.

A parametric study showed that $\phi = 0.5$ is the best choice; this value is adopted as a constant of the model.

Conclusions

A k-ϵ formulation has been developed for turbulence modeling within wall-bounded two-dimensional separation bubbles. The model is based on experimental obsevations. Two basic features of the model are: 1) turbulence kinetic energy within the backflow region is a Gaussian function of the distance from the wall; 2) the length scale of turbulence within the bubble is proportional to the local distance from the wall to the edge of the viscous sublayer located outside the backflow region. The formulation enables unified k-ϵ modeling between the wall and the viscous sublayer edge.

The model has been preliminarily validated through comparisons with data, and will be incorporated into a Reynolds-averaged Navier-Stokes solver to calculate flowfields where separated regions may occur.

References

[1]Simpson, R. L., "Some Features of Two-Dimensional Turbulent Separated Flows," AIAA Paper 85-0178, Jan. 1985.

[2]Simpson, R. L., "A Review of Some Phenomena in Turbulent Flow Separation," *Transactions of ASME*, Vol. 103, Dec. 1981, pp. 520-533.

[3]Simpson, R. L., Chew, Y.-T., and Shivaprasad, B. G., "The Structure of a Separating Turbulent Boundary Layer. Part 1, Mean Flow and Reynolds Stresses," *Journal of Fluid Mechanics*, Vol. 113, Dec. 1981, pp. 23-51.

[4]Délery, J. M., "Experimental Investigation of Turbulence Properties in Transonic Shock/Boundary-Layer Interations," *AIAA Journal*, Vol. 21, Feb. 1983, pp. 180-185.

[5]Gorski, J. J., "A New Near-Wall Formulation for the k-ϵ Equations of Turbulence," AIAA Paper 86-0556, Jan. 1986.

Measurement of the Speed of Sound in Ice

Alphonso C. Smith* and Doron Kishoni†
NASA Langley Research Center, Hampton, Virginia

Introduction

SOUND-speed measurements in refrigerated ice have been determined by using pulse-echo ultrasonic applications. For these measurements, two parameters were important for accuracy, namely, the ice thickness and the time required for

Received Feb. 11, 1986; revision received March 27, 1986.

*Research Scientist, Instrument Research Division.
†NRC Research Associate.